Calculated One-Electron Reduction Potentials and Solvation Structures for Selected *p*-Benzoquinones in Water

Kevin S. Raymond, Anthony K. Grafton, and Ralph A. Wheeler*

Department of Chemistry and Biochemistry, University of Oklahoma, 620 Parrington Oval, Room 208, Norman, Oklahoma 73019

Received: June 20, 1996; In Final Form: November 20, 1996[⊗]

The one-electron reduction of quinones is important not only in electrochemistry but also in biochemical energy storage, energy utilization, and organic chemcial reactions. Thermodynamic cycles are investigated to estimate aqueous one-electron reduction potentials for the redox indicators *p*-benzoquinone and *p*-duroquinone, as well as chloro-substituted *p*-benzoquinones. Gas-phase reduction free energy differences are approximated from electron affinities calculated by using the hybrid Hartree−Fock/density-functional B3LYP method, a semiempirical quantum chemical method that expresses a molecule's exchange-correlation energy as a weighted sum of Hartree−Fock, local, and gradient-corrected density-functional energies. Free energy perturbation theory was used with molecular dynamics simulations (at constant temperature, pressure, and number of atoms) to estimate hydration free energy differences. Calculated one-electron reduction potentials for the quinones are within 10−190 meV of experimental values. An exceptionally accurate reduction potential was calculated for *p*-benzoquinone ($E^0_{calc} = 4.51$ eV and $E^0_{expt} = 4.52$ to 4.54 eV) and least accuracy was obtained for *p*-duroquinone ($E^0_{calc} = 3.99$ eV and $E^0_{expt} = 4.18-4.21$ eV). Radial distribution functions show that more hydrogens contact the oxygens of the *p*-benzosemiquinone anions than the oxygen atoms of the neutral quinones. The strengths and numbers of water hydrogen bonds to the semiquinone anions also correlate with hydration free energy differences between the quinones and their semiquinone anions, implying that models of water solvation designed to reproduce hydration free energy differences or reduction potentials should somehow incorporate the effects of specific solute−water interactions.

Introduction

The gain or loss of a single electron by a neutral molecule to form the corresponding anion or cation radical is a fundamental chemical reaction. Its importance transcends electrochemistry[1,2] and encompasses organic, inorganic, and biochemical reactions.[3] For example, many enzymes function by electron transfer (ET), and indeed, ET is a basic step in the storage and utilization of energy by living organisms.[4,5] Early studies of ET concerned the oxidation−reduction chemistry of metal complexes[6] so that ET now occupies a prominent place in the literature of inorganic chemistry.[3,7] In organic chemistry, even the classical S_N2, Diels−Alder, and electrophilic aromatic substitution reactions have recently been cast in terms of single electron transfer events.[8,9]

Despite the importance of ET, calculating the free energy (alternatively, the reduction potential) for one-electron reductions remains a challenging problem that requires accurately modeling energy changes due to changes in intramolecular bonding and changes in molecular solvation. A variety of methods have been proposed to address these and related issues, ranging from empirical correlations between gas-phase electron affinities and reduction potentials in aprotic solvents[10−12] to more general methods of *ab initio* molecular dynamics calculations.[13−20] A recently proposed method of intermediate complexity uses thermodynamic cycles to separate the calculation of solute bond energy changes from solvation free energy changes.[21,22,82] Although the force field neglects polarizability, the original implementation yields a very accurate one-electron reduction potential for aqueous *p*-benzoquinone, **1a**,[21] thus demonstrating the feasibility of thermodynamic cycle/free energy perturbation theory[23−31] for the computer-aided design of molecules and their solvent surroundings with predictable electrochemical properties. Since the completion of the aforementioned work, we have further tested the proposed methods and extended them to other hydrated quinone systems of chemical importance,[4,32−34] including *p*-benzoquinone (**1a**), *p*-duroquinone (**1b**), and a variety of chloro-substituted quinones, such as *p*-chloranil (**1c**). In addition, we have analyzed the hydration structures of the quinones and their semiquinone anions (representative resonance structures are shown in Scheme 1) to determine the specific intermolecular contacts most important for stabilizing the hydrated molecules and anions.

The quinones were chosen to test the method because of their ubiquitous presence in ET chemistry:[35] *p*-benzoquinone and *p*-duroquinone are commonly used as aqueous redox indicators,[36] whereas *p*-chloranil is an important oxidant in organic chemistry[32] and the chloro-substituted *p*-benzoquinones are less symmetrical, related structures. Experimental values of the one-electron reduction potentials for *p*-benzoquinone and *p*-duroquinone in water are thus known very precisely.[36] *p*-Chloranil, on the other hand, reacts rapidly with water, and its reduction potential has been determined only indirectly.[37] The quinones selected as test molecules should also exhibit a variety of solvation structures and present several different computational challenges. First, they possess dipole moments of varying magnitudes due to their different substituent positions. Moreover, the size of the chloro and methyl substituents are similar, but they are electronically very different. The methyl group is electron donating, whereas the highly electronegative chloro substituent withdraws electron density from the σ system of the quinone, while its lone-pair electrons serve as weak π donors. Before presenting calculated one-electron reduction potentials and comparing hydration structures for the species

[⊗] Abstract published in *Advance ACS Abstracts,* January 1, 1997.

S1089-5647(96)01852-4 CCC: $14.00

SCHEME 1

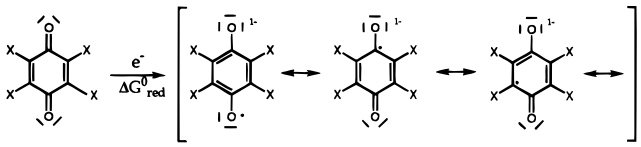

1a: X = H for *p*-benzoquinone/*p*-benzosemiquinone anion
1b: X = CH_3 for duroquinone/durosemiquinone anion
1c: X = Cl for *p*-chloranil/*p*-chloranil anion

SCHEME 2

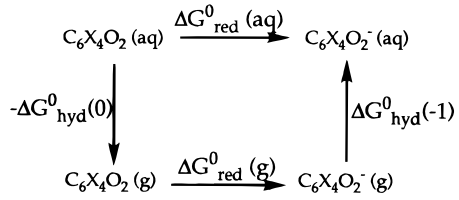

considered, we discuss the thermodynamic cycles that form the basis for the computational method.

Thermodynamic Cycles

One way to analyze the one-electron reduction of a quinone to its semiquinone anion is demonstrated by the thermodynamic cycle shown in Scheme 2. The top reaction in the cycle represents the reduction of a quinone to its semiquinone anion in aqueous solution, characterized by a Gibbs free energy of reduction, $\Delta G^0_{red}(aq)$. An alternate path from reactant to product is represented in Scheme 2 by quinone desolvation, gas-phase reduction, and solvation of the semiquinone anion. Since free energy is a state function, the sum of free energies for the two paths from reactants to products must be equivalent. The cycle shown in Scheme 2 can therefore be used by (1) equating the reduction free energy in water to the sum of free energies for the indirect route from reactants to products, $\Delta G^0_{red}(aq) = \Delta G^0_{red}(g) + \{\Delta G^0_{hyd}(-1) - \Delta G^0_{hyd}(0)\}$ and (2) relating the standard Gibbs free energy of reduction, $\Delta G^0_{red}(aq)$, to the standard one-electron reduction potential, E^0, by $\Delta G^0_{red}(aq) = -FE^0$, where F is the Faraday constant ($F = 23.06$ kcal mol^{-1} V^{-1}). The inability of molecular dynamics (MD) simulations with empirical potentials to calculate accurate gas-phase free energy changes due to changes in intramolecular bonding, $\Delta G^0_{red}(g)$, and the excessive computer time necessary to use quantum chemical methods to calculate hydration free energy differences, $\{\Delta G^0_{hyd}(-1) - \Delta G^0_{hyd}(0)\}$, for such a large system make the exclusive use of either calculation method impractical. However, by incorporating a combination of MD methods to calculate hydration free energy differences and quantum chemical methods to approximate gas-phase reduction free energies as calculated electron affinities, one may use the above thermodynamic cycle to estimate the standard Gibbs free energy of reduction and therefore the standard reduction potential. Scheme 3 shows an alternate thermodynamic cycle useful for calculating the standard free energy of reduction. This cycle relates the hydration free energy difference between *p*-benzoquinone and *p*-benzosemiquinone anion, $\Delta\Delta G^0_{hyd} = \Delta G^0_{hyd}(-1) - \Delta G^0_{hyd}(0)$, to the same quantity for other quinones. Since no transformations in Scheme 3 require an overall change in molecular charge, corrections to account for neglecting long-range Coulombic interactions, such as the Born charging correction,[38−40] are not necessary for these portions of the cycle. Instead, the charging correction is already incorporated in the previously calculated quantities for the reduction of *p*-benzoquinone to *p*-benzosemiquinone anion, which agree well with experimental values. The hydration free energy difference

SCHEME 3

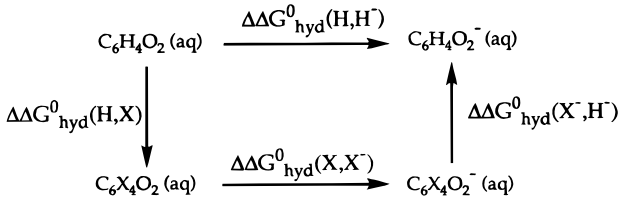

between a quinone and its semiquinone anion may then be described by the following relation, taken from the cycle in Scheme 3:

$$\Delta\Delta G^0_{hyd}(X, X^-) = \Delta\Delta G^0_{hyd}(H, H^-) + \{\Delta\Delta G^0_{hyd}(H, X) + \Delta\Delta G^0_{hyd}(X^-, H^-)\}$$

$\Delta\Delta G^0_{hyd}(X, X^-) = \Delta G^0_{hyd}(-1) - \Delta G^0_{hyd}(0)$ may then be substituted back into the cycle in Scheme 2 to calculate the standard Gibbs free energy of reduction and the standard reduction potential for any substituted *p*-benzoquinone. Of course, the cycles shown above could equally well refer to solvents other than water or to inhomogeneous media such as proteins.

Calculated Energy Differences

To estimate gas-phase reduction free energy differences, electron affinities were calculated by using the B3LYP hybrid Hartree−Fock/density-functional (HF/DF) method.[41,42] The method expresses a molecule's energy as a weighted sum of Hartree−Fock exchange (E_X^{HF}) and density-functional exchange-correlation energies. Density-functional approximations for the exchange-correlation energy, $E_{XC}(\rho)$, employed in the B3LYP method include Slater's local (E_X^{Slater})[43] and Becke's gradient-corrected (E_X^{Becke})[44] exchange energies, combined with the local correlation energy expression of Vosko, Wilk, and Nusair (E_C^{VWN})[45] and the nonlocal, gradient-corrected correlation energy proposed by Lee, Yang, and Parr (E_C^{LYP}).[46] The B3LYP expression for a molecule's exchange-correlation energy is therefore

$$E_{XC}(\rho) = AE_X^{Slater} + (1 - A)E_X^{HF} + BE_X^{Becke} + CE_C^{LYP} + (1 - C)E_C^{VWN}$$

where $A = 0.80$, $B = 0.72$, and $C = 0.81$. The parameters A, B, and C were chosen by Becke to reproduce heats of formation for a set of small molecules, for the case where Perdew's 1986 correlation functional[47] replaces the LYP functional.[48,49] Although these same parameters A, B, and C may not be entirely appropriate when the LYP gradient-corrected correlation functional is used, tests by Bauschlicher and Partridge demonstrate the B3LYP method's thermochemical accuracy.[50,51] We have subsequently shown that the B3LYP method with a 6-311G-(3d,p) basis set gives electron affinities within an average absolute magnitude of 0.05 eV of experimental values for a number of methylated and halogenated *p*-benzoquinones, including those discussed here.[52] Of course, the electron affinity properly approximates only the reduction enthalpy and neglects entropic contributions to the gas-phase reduction free energy. Published experiments nonetheless indicate that the gas-phase reduction enthalpy represents all but approximately 0.04 eV of the gas-phase reduction free energy for *p*-benzoquinones.[10,53]

The free energy perturbation (FEP) method with molecular dynamics was chosen to calculate hydration free energy differences because it yields accurate hydration free energy differences between various organic and biological molecules

and between halide ions and noble gas atoms.[23−31] The FEP method was developed to minimize numerical errors by expressing the Hamiltonian, or energy operator, as a weighted sum of Hamiltonians for reactants and products. To change a quinone into its semiquinone anion, the Hamiltonian is therefore a weighted sum of the Hamiltonians appropriate for the neutral quinone and its anion:

$$H_\lambda = \lambda H(C_6X_4O_2^-) + (1 - \lambda)H(C_6X_4O_2)$$

In our FEP calculations, the parameter λ was varied from 0 to 1 in small increments, referred to as "windows", as the geometry and MD parameters for a neutral quinone were changed to those for the corresponding semiquinone anion. The reported free energy difference between each quinone and its semiquinone anion is a sum of small equilibrium free energy changes calculated for each of 20 identical windows of a fixed size. For each quinone a second, independently equilibrated sample containing the semiquinone anion was transformed into one containing the corresponding quinone and the magnitude of the free energy changes for forward and reverse simulations was averaged to give the reported free energy difference. The difference between the average free energy change and the free energy change from either simulation is a lower limit for the error.

Simulations were thus performed for a constant pressure, temperature, and number of atoms by using the AMBER MD programs.[54] A temperature of 300 ± 20 K and a pressure of 1 atm were maintained by coupling the system to external temperature and pressure baths with a time constant of 0.1 ps.[55,56] Bond distances were held constant by using the SHAKE coordinate resetting algorithm[57,58] to allow use of a 0.001 ps time step, and all structures were equilibrated for at least 100 ps before beginning FEP calculations. A single molecule or ion was solvated by 647 TIP3P water molecules[59] in a rectangular box incorporating periodic boundary conditions. Interactions in solution were cut off beyond 10 Å, and a Born charging correction[38−40] of 16.35 kcal mol^{-1} was applied by using the first term from eq 15 of ref 61, a multipole expansion of the energy for a distribution of charges within a sphere imbedded in a structureless, polarizable dielectric.[60,61] For molecules with a permanent dipole moment, the dipolar term in the multipole expansion was calculated, but its magnitude is less than 0.01 eV. Although the truncated multipole expansion is an approximation, higher-order terms in the expansion for the substituted *p*-benzoquinone derivatives in water are likely to be even smaller. Terms in the expansion of higher order than the order of the dipolar term fall off as $1/r^5$ or faster and are therefore likely to be insignificant for the cutoff distance employed. The 10 Å radius of the sphere was used as the cutoff distance and the dielectric constant was assumed to be the same as the experimental dielectric constant of water, 78.

Because truncation of long-range interactions and use of the Born correction are approximations, a large amount of work has been done to test its accuracy and to investigate alternatives such as generalized reaction field methods and Ewald sums.[62−70] Although Ewald sums are generally more accurate, especially for calculating potentials of mean force for ion pairs,[68,71] the Born charging correction reportedly recaptures approximately 95−98% of the hydration free energy lost by cutting off interactions between a single ion and distant water molecules.[72−74] We have nonetheless investigated ways to attenuate the effects of cutoffs on calculated energy differences by considering thermodynamic cycles involving species of the same charge, such as that shown in Scheme 3. The simulations involved in calculating energies for the cycle shown in Scheme 3 were done similarly to those described above. FEP/MD simulations were accomplished by transforming one quinone into another and one semiquinone anion into the other, and the hydration free energy differences were combined to yield the reported hydration free energy difference between a substituted *p*-benzoquinone and its semiquinone anion. The calculated hydration free energy differences were then used in eq 1 to estimate the one-electron reduction potentials for the substituted *p*-benzoquinones.

The Gibbs hydration free energy differences between the quinones and their semiquinone anions, $\Delta\Delta G^0_{hyd} = \Delta G^0_{hyd}(-1) - \Delta G^0_{hyd}(0)$, were actually estimated from two sets of the FEP/MD simulations indicated in Schemes 2 and 3. The simulations utilized in Scheme 2 transformed a quinone into its semiquinone anion in the gas phase (to estimate intramolecular interactions, $\Delta G^0_{red}(g)$) and in water (to calculate $\Delta G^0_{red}(aq)$). According to the thermodynamic cycle shown in Scheme 2, the difference between the aqueous and gas-phase energies is the hydration free energy difference $\Delta\Delta G^0_{hyd}$. Gas-phase MD simulations were thus performed in the same way as the solution simulations except that because no periodic boundary conditions were implemented, cutting off interactions beyond specified distances was unnecessary and the Born correction was not needed.

Energies calculated by using molecular dynamics methods were derived from kinetic energies and potential energy expressions for interactions between atom pairs−including Lennard-Jones and Coulombic nonbonded terms, harmonic bond angle bending, and sinusoidal torsional angle-twisting terms. Although some MD force fields include explicit terms to account for hydrogen bonding,[54] we elected to allow hydrogen-bonding interactions to arise naturally out of a combination of Coulombic and Lennard-Jones interactions. For water, the well-known TIP3P model[59] was used, and for quinones, Lennard-Jones parameters were adopted from those for similar atom types in the work of Weiner, Kollman et al.[75,76] Other force field parameters for the quinones and semiquinone anions were derived by using the GAUSSIAN92/DFT computer programs,[41] hybrid HF/DF quantum chemical methods,[41,42,49] and a 6-31G(d) basis set. The particular method and basis set were chosen because they yield extremely accurate structures for *p*-benzoquinones[77] and harmonic vibrational frequencies accurate to within an average of approximately 20−50 cm^{-1} for a number of organic π radicals,[78−80] *p*-benzoquinones,[77,81,82] and *p*-benzosemiquinone radical anions.[81,82] Apparently, anharmonic corrections for these species are small and the three-parameter, HF/DF methods show considerable promise for providing accurate harmonic force fields. We note that accurately approximating the effects of electron correlation on molecular charge distributions is important not only for determining partial atomic charges, but also for calculating accurate vibrational frequencies, and vibrational force constants,[83,84] for radicals and radical anions. Thus, hybrid HF/DF methods were used to calculate harmonic force constants for the various quinones and semiquinone anions[77,85] because they provide an economical way to incorporate electron correlation. Harmonic force constants were derived from HF/DF calculations by using internal coordinates chosen according to the procedure recommended by Boatz and Gordon.[86] For torsional angle twisting, the harmonic force constants were adapted for use in AMBER by using a trigonometric identity to relate the functional form of the AMBER torsional potential, $V_n/2\{\cos(n\phi - \phi_0)\}$, to sines and cosines of the individual angles $n\phi$ and ϕ_0. Since the equilibrium torsional angle ϕ_0 is 180° for each torsional angle required, expanding cos $n\phi$ in a Taylor series gives the

TABLE 1: Hydration Free Energy Differences between Tetrachloro-*p*-benzoquinone and Its Semiquinone Anion[a] Derived from Thermodynamic Cycle in Scheme 2 and Hydration Free Energy Differences Used To Derive the Same Quantity Using Thermodynamic Cycle in Scheme 3

simulation[b]	$\Delta\Delta G^0_{hyd}$ (kcal/mol) 2500 steps/window[c]	$\Delta\Delta G^0_{hyd}$ (kcal/mol) 5000 steps/window[c]	$\Delta\Delta G^0_{hyd}$ (kcal/mol) 15 000 steps/window[c]
TClQ/TClSQ$^{\bullet-}$	−45.22	−47.31	−47.35
TClSQ$^{\bullet-}$TClQ	44.86	46.50	47.87
PBQ/PBSQ$^{\bullet-}$	−60.98	−59.95	−61.24
PBSQ$^{\bullet-}$/PBQ	58.62	59.54	61.41
TClQ/PBQ	2.09	2.99	3.38
PBQ/TClQ	−3.12	−3.19	−3.31
TClSQ$^{\bullet-}$/PBSQ$^{\bullet-}$	−11.55	−11.06	−11.66
PBSQ$^{\bullet-}$/TClSQ$^{\bullet-}$	11.35	10.79	11.71

[a] Experimentally derived $\Delta\Delta G^0_{hyd}$ values calculated as the difference between the measured one-electron reduction potentials and electron affinities (see Table 2) are 44.97 kcal/mol and 61.57−62.03 kcal/mol for TClQ and PBQ respectively. [b] TClQ and TClSQ$^{\bullet-}$ here stand for tetrachloro-*p*-benzoquinone (*p*-chloranil) and its semiquinone radical anion. [c] Each window used a 2:3 ratio of the number of equilibration steps to the number of data gathering steps.

approximate relation $V_n/2 = K_\phi/n^2$, where K_ϕ are the harmonic force constants obtained from HF/DF calculations. Atomic charges were also derived from HF/DF calculations[48,49] of the electrostatic potential on a grid of approximately 9000 points, spaced 0.3 Å apart and located outside the van der Waals radius of each atom, but within 2.8 Å of any atom. Then, the least-squares fitting program CHELPG[87,88] was used to determine the partial atomic charges that best reproduce the electrostatic potential on the grid of points.

Table 1 presents Gibbs hydration free energy differences between quinoidal species derived from FEP/MD simulations. The table's first four rows display the hydration free energy differences between tetrachloro-*p*-benzoquinone (or *p*-chloranil, abbreviated TClQ) and its semiquinone anion (TClSQ$^{\bullet-}$) and between *p*-benzoquinone and its anion. The data necessary to calculate the hydration free energy difference between *p*-chloranil and its anion by using the cycle Scheme 3 are also listed in the table. Calculated hydration free energy differences displayed in Table 1 were calculated for both forward and reverse directions at constant temperature and pressure, using a variety of different simulation times. The calculated hydration free energy difference between each pair of molecules is simply the average of the values for forward and reverse simulations. Because the calculated Gibbs hydration free energy differences presented in Table 1 are similar for total simulation times varying from 25 ps (2500 steps per window) to 150 ps (15 000 steps per window), calculations appear to be converged. To further test convergence of the FEP/MD calculations for *p*-benzoquinone, simulations of 450 ps (45 000 steps per window) were performed. The average hydration free energy difference for the forward and reverse calculations from the 450 ps simulation, 60.24 kcal mol^{-1}, is within 1.1 kcal mol^{-1} of the calculated average for the 150 ps simulation listed in the table. For the longest simulation times shown in the table, the differences between free energies calculated in the forward and reverse directions and their average magnitudes are less than 0.3 kcal mol^{-1}, so systematic errors also appear small. Finally, summing numbers in the last three pairs of rows in the table according to the thermodynamic cycle Scheme 3 gives an average hydration free energy difference for *p*-chloranil of 46.30 kcal mol^{-1}, within 1.31 kcal mol^{-1} of the average from the cycle in Scheme 2 (47.61 kcal mol^{-1}). Thus, Schemes 2 and 3 give very similar values for the hydration free energy difference between *p*-chloranil and its semiquinone anion.

Table 2 shows experimental one-electron reduction potentials for a variety of substituted *p*-benzoquinones,[2,36,37,89−91] reduction potentials calculated by using the thermodynamic cycles shown in Schemes 2 and 3, Gibbs hydration free energy differences for various quinone/semiquinone anion couples, electron affinities calculated by using the B3LYP/6-311G(3d,p) method,[52] and experimental electron affinities.[10,53,92,93] Experimental absolute reduction potentials for the various quinones were obtained by following the current IUPAC recommendation[94] to add 4.44 ± 0.02 V to the experimental reduction potentials measured relative to the normal hydrogen electrode. The calculated one-electron reduction potential shown in the table for each quinone is obtained by adding the calculated electron affinity to the hydration free energy difference between the quinone and its semiquinone anion, obtained by using the appropriate thermodynamic cycle. The cycle in Scheme 3 attempts to minimize the influence of the Born charging correction by combining the very accurate reduction potential for *p*-benzoquinone/*p*-benzosemiquinone anion with perturbations that do not entail changing molecular charges.

Both the calculated electron affinities and one-electron reduction potentials listed in Table 2 agree very well with experimental values. Except for *p*-benzoquinone and 2,6-dichloro-*p*-benzoquinone, calculated electron affinities overestimate experimental values by 0.01−0.21 eV. The two largest differences between experimental and calculated electron affinities evident in the table, 0.21 and 0.14 eV, arise for molecules whose electron affinities were estimated from charge transfer spectra, so their computed electron affinities may be more accurate than the table indicates.[52] The differences between experimentally measured reduction potentials[2,36,37,89−91] and our

TABLE 2: Experimental[2,36,37,89−91] and Calculated Absolute One-Electron Reduction Potentials (E^0), Hydration Free Energy Differences between Various Quinones and Their Semiquinone Anions, ($\Delta\Delta G^0_{hyd}$) and Calculated[52] and Experimental[10,53,92,93] Electron Affinities (EA)

compound	exptl E^0 (eV ± 0.050)	calculated E^0 using Scheme 2 (eV)[a,b]	calculated E^0 using Scheme 3 (eV)	calculated $\Delta\Delta G^0_{hyd}$ from Sch eme 2 (eV)	calculated $\Delta\Delta G^0_{hyd}$ from Scheme 3 (eV)	calculated EA (ev)	exptl EA (eV ± 0.10)
PBQ	4.52−4.54	4.51 ± 0.01		2.66		1.85	1.91
p-chloranil	4.78	4.90 ± 0.01	4.84 ± 0.01	2.07	2.01	2.83	2.78
trichloro-PBQ		4.80 ± 0.01	4.84 ± 0.01	2.13	2.17	2.67	2.56
2,3-dichloro-PBQ		4.70 ± 0.01	4.72 ± 0.01	2.30	2.32	2.40	2.19 ± 0.15
2,5-dichloro-PBQ	4.65	4.66 ± 0.02	4.53 ± 0.02	2.18	2.05	2.48	2.44
2,6-dichloro-PBQ	4.65	4.72 ± 0.01	4.65 ± 0.04	2.24	2.28	2.48	2.48
chloro-PBQ		4.62 ± 0.01	4.40 ± 0.01	2.43	2.21	2.19	2.05 ± 0.15
p-duroquinone	4.18−4.21	3.99 ± 0.01	3.95 ± 0.04	2.36	2.32	1.63	1.62

[a] Calculated E^0 values may be obtained by adding the $\Delta\Delta G^0_{hyd}$ value from the appropriate cycle to the calculated electron affinity. [b] Errors reported for calculated E^0's should be taken as lower bounds on the actual errors and were obtained by taking one-half the difference between the forward and reverse simulations.

best calculated results vary from 10 to 30 mV for *p*-benzoquinone to the largest errors of 190−220 mV for *p*-duroquinone. The accuracy obtained by using the cycle in Scheme 2 is actually slightly better than that for the cycle in Scheme 3. Except for *p*-duroquinone, errors in calculated hydration free energy differences between each quinone and its semiquinone anion are similar in magnitude to errors in calculated electron affinities, but no systematic direction for the error in calculated hydration free energies is evident. To test the possibility that the error in the calculated hydration free energy difference between *p*-duroquinone and its semiquinone anion using thermodynamic cycle in Scheme 3 may result from changes in solute size upon perturbing from *p*-benzoquinone/*p*-benzosemiquinone anion to *p*-duroquinone/*p*-durosemiquinone anion, further studies using the thermodynamic cycle in Scheme 3 and perturbing between *p*-duroquinone and *p*-chloranil were performed. We also performed FEP/MD simulations for *p*-duroquinone using an all-atom model for the molecule's methyl groups, but unfortunately neither set of simulations improved the accuracy of the calculated reduction potential for *p*-duroquinone. We note that all FEP/MD simulations reported in the tables were obtained by using the "single-wide" sampling option of the AMBER programs,[54] but calculations using "double-wide" sampling for *p*-duroquinone and *p*-benzoquinone gave virtually identical results.[95]

Hydration Structures

Tables 1 and 2 demonstrate that hydration free energy differences make a contribution to the Gibbs reduction free energies for the *p*-benzoquinones studied comparable to that of the electron affinities. Because hydration free energy differences should depend on the extent of solvent reorientation upon going from the neutral quinone to the reduced semiquinone anion, we have investigated changes in hydration structures by analyzing a number of radial distribution functions.[96,97] Various factors influence solvent structure, but we note that our simulations include no special parameters to describe hydrogen bonding, so any hydrogen-bonding interactions must arise from a combination of electrostatic and Lennard-Jones interactions between solute−solvent and solvent−solvent atom pairs. Figures 1−4 therefore show various radial distribution functions for the *p*-benzoquinone/*p*-benzosemiquinone anion systems. All radial distribution functions presented here are averages of at least 5000 independent structures obtained 0.010 ps apart during an MD run with λ held constant at one end point of the simulation. In addition to equilibration of the systems for FEP/MD simulations, each system was equilibrated for at least 100 ps before beginning data acquisition for the radial distribution functions. We focus first on *p*-benzoquinone and its anion because other radial distribution functions show similar features.

Figure 1 compares the quinone oxygen−water hydrogen radial distribution functions for *p*-benzoquinone and *p*-benzosemiquinone anion. For *p*-benzosemiquinone anion, the first sharp peak in the radial distribution function appears near a distance of 1.6 Å, with a smaller, less pronounced peak near 3.0 Å. The second peak in the oxygen−hydrogen radial distribution function near 3.0 Å appears at a distance appropriate for the second hydrogen of the water in close contact with the quinone oxygen and does not indicate a second hydration shell. Instead, these two peaks together arise primarily from water molecules within the first solvation shell. The deep minimum separating the two peaks implies little exchange of the two hydrogen atoms within the first coordination shell. In contrast, the first peak in the quinone oxygen−water hydrogen radial distribution function for *p*-benzoquinone appears at a slightly

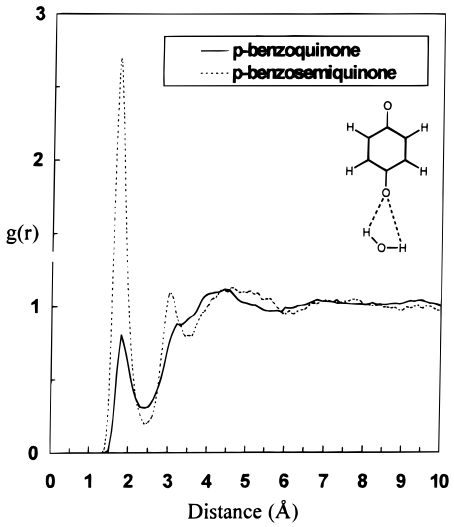

Figure 1. Quinone oxygen−water hydrogen radial distribution functions illustrating the larger number of close contacts with water for *p*-benzosemiquinone anion compared to neutral p-benzoquinone. The schematic structure in the upper right indicates the atoms used to plot $g(r)$ and is not meant to imply a rigid coordination geometry.

longer distance, 1.8 Å, and has a much smaller magnitude. Furthermore, the second peak, near 3.1−3.4 Å, is broad and indistinct with only a relatively shallow minimum separating the two peaks. The interactions between the oxygen atoms of *p*-benzosemiquinone anion or *p*-benzoquinone and the solvent hydrogen therefore show distinct differences. Integrating the radial distribution functions to the first minimum using the trapezoid rule shows that the more negatively charged oxygen atoms of *p*-benzosemiquinone anion interact with a greater number of solvent molecules (an average of approximately 3.3), at a smaller distance, than the oxygens of *p*-benzoquinone (an average of approximately 1.7). Although they are not shown, quinone oxygen−water hydrogen radial distribution functions for the other *p*-benzoquinones shown in Table 2, and their anions, display trends that are similar to but less pronounced than those shown in Figure 1. The semiquinone anions are thus more strongly solvated, by more water molecules, than their respective neutral quinones.

The quinone oxygen−water oxygen radial distribution functions for *p*-benzosemiquinone anion and *p*-benzoquinone displayed in Figure 2 provide further geometrical information concerning the quinone oxygen−water interactions. The first peak in the oxygen−oxygen radial distribution function for *p*-benzosemiquinone anion appears at 2.5−2.6 Å, well within the sum of van der Waals radii for the two oxygens, and a broader peak is evident at 4.4 Å. The difference between the positions of the first peaks in the oxygen−oxygen and oxygen−hydrogen radial distribution functions, 0.9−1.0 Å, corresponds to the oxygen−hydrogen distance for TIP3P water[59] and thus indicates a nearly linear O···H−O geometry. The linear O···H−O geometry and the 1.6 Å distance between the *p*-benzosemiquinone anion's oxygens and water hydrogens are consistent with crystallographic evidence of hydrogen bonding,[98−100] even though no special interaction parameters were included in the calculation to represent hydrogen bonding. Instead, the stronger hydrogen bonding of semiquinone anion oxygens with water appears to result from the large difference in negative charge on the oxygen atoms of the two species (*p*-benzosemiquinone anion oxygens are more negative by 0.17 electrons than the oxygens of the neutral molecule). Furthermore, the second broad peak at 4.4 Å indicates a possible second solvation shell. This second peak in the quinone oxygen−water

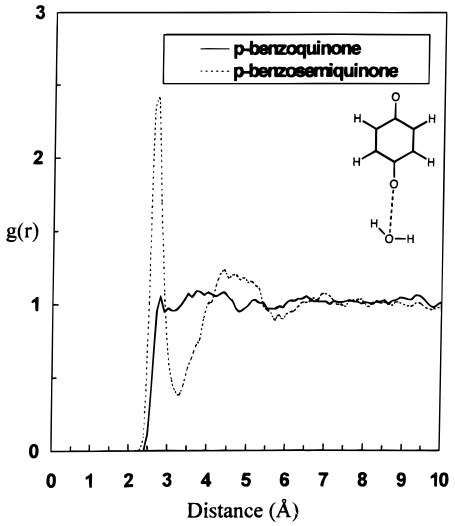

Figure 2. Quinone oxygen−water oxygen radial distribution functions for *p*-benzoquinone and *p*-benzosemiquinone anion. The sharper anion peak implies a more ordered first solvation shell, and the second, broad peak near 4.4 Å implies a possible second solvation shell for the anion.

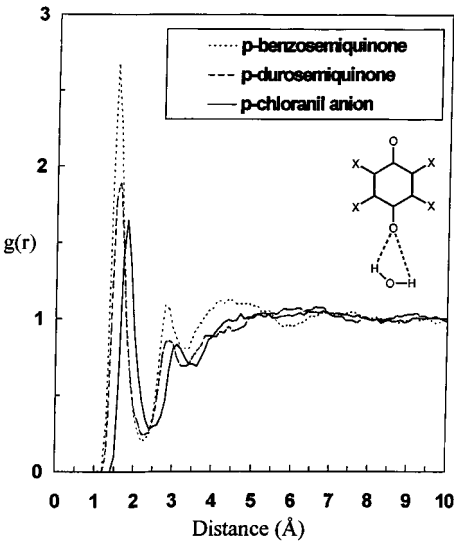

Figure 3. Quinone oxygen−water hydrogen radial distibution functions for the anions for *p*-benzoquinone, *p*-duroquinone, and *p*-chloranil. Closer, higher peaks imply stronger interaction with water and correlate with larger calculated hydration free energy differences between the anion and its neutral quinone. The schematic structure in the upper right indicates the atoms used to plot $g(r)$ and is not meant to imply a rigid coordination geometry.

oxygen radial distribution function for all three semiquinone anions is not present for the neutral quinones and implies that electrostriction−solvent density variations due to the electrostatic field of the semiquinone anions−also contributes to hydration free energy differences between the quinones and their semiquinone anions.

Figure 3 compares the quinone oxygen−water hydrogen radial distribution functions for the anions of *p*-benzoquinone, *p*-duroquinone, and *p*-chloranil. This figure shows that the trend in anion oxygen−water hydrogen distances, the number of anion oxygen−water hydrogen contacts, and the rigidity of the first solvation shell is *p*-benzosemiquinone anion ≫ *p*-durosemiquinone anion > *p*-chloranil anion. Although it is impossible to separate rigorously the effects of electrostatics from sterics, the similar peak heights for *p*-durosemiquinone and *p*-chloranil anions arise primarily because of their similar charges (oxygen charges are the same within 0.003 electrons). In contrast, the closer first peak for the *p*-durosemiquinone anion in Figure 3

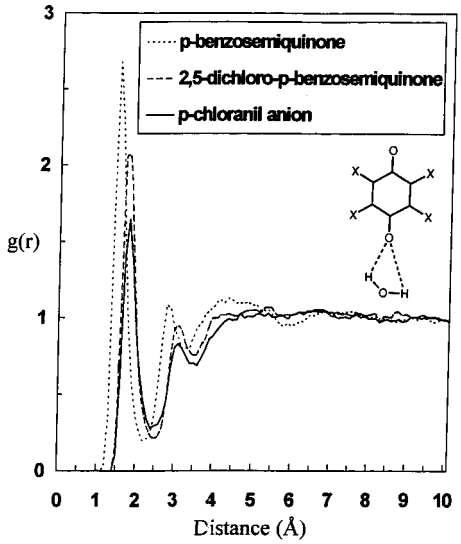

Figure 4. Quinone oxygen−water hydrogen radial distribution functions for the anions for *p*-benzoquinone, 2,5-dichloro-*p*-benzoquinone, and *p*-chloranil. Closer, higher peaks imply stronger interaction with water and correlate with larger calculated hydration free energy differences between the anion and its neutral quinone. The schematic structure in the upper right indicates the atoms used to plot $g(r)$ and is not meant to imply a rigid coordination geometry.

appears to arise mainly from the smaller steric bulk of methyl compared to chloro substituents, expressed by its shallower Lennard-Jones potential well. We also note that the trends described above correspond to the trend in calculated Gibbs hydration free energy differences for the various quinone/semiquinone anion couples, listed in Tables 1 and 2.

Finally, Figure 4 compares quinone oxygen−water hydrogen radial distribution functions for the anions of *p*-benzoquinone, 2,5-dichloro-*p*-benzoquinone, and *p*-chloranil and illustrates the effect of increasing the number of chlorine atoms adjacent to the semiquinone anion's oxygen atoms. Of the three semiquinone anions, the *p*-benzosemiquinone anion's oxygens experience the most close contacts with water hydrogens at the shortest distance. The two added chlorine atoms of 2,5-dichloro-*p*-benzosemiquinone anion apparently exclude some waters from close contact with the anion's oxygens, since the first peak in the radial distribution function appears at a larger distance, whereas the *p*-chloranil anion's oxygen atoms show the fewest close contacts with water.

Radial distribution functions between water hydrogens, water oxygens, and the other atoms of the various quinones and semiquinone anions were also calculated but showed no pronounced structure comparable to that between quinone oxygens and the atoms of water. In particular, the hydrogen, chlorine, and methyl quinone substituents show negligible differences in hydration structures between the quinones and their semiquinone anions, between the different quinones, or between the semiquinone anions. For all the quinones studied here, the hydrogen and oxygen atoms of water closest to the quinone substituents are located further than the sum of the van der Waals radii. Furthermore, the water hydrogens adopt poorly defined geometries and indicate little orientational ordering.

To investigate the energetic consequences of the close contacts evident in the radial distribution functions, Figure 5 was constructed to show the average interaction energy of solvent water molecules with the negatively charged oxygens of *p*-benzosemiquinone, *p*-durosemiquinone, and *p*-chloranil radical anions versus distance between solvent and solute oxygens. The energy was calculated according to the AMBER force field form (eq 1 of ref 76 without the hydrogen bonding

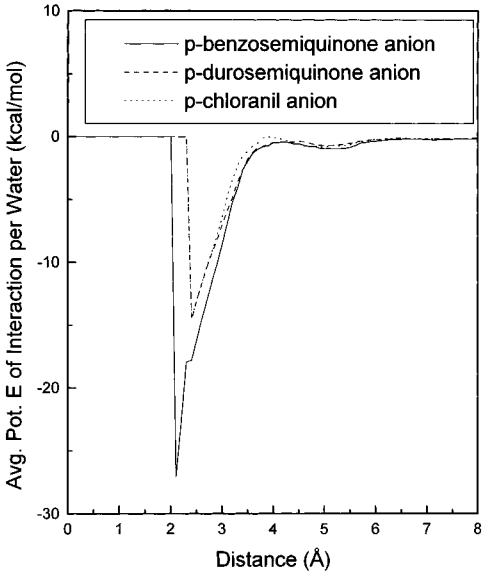

Figure 5. Average potential energy of interaction, per water molecule, between the negatively charged oxygen atoms of *p*-benzosemiquinone, *p*-durosemiquinone, and *p*-chloranil anions and the atoms of water as a function of semiquinone oxygen−water oxygen distance.

term) and averaged over at least 2500 independent, equilibrium structures. Therefore, the plot in Figure 5 gives no indication of the *number* of waters at a particular distance (for this information, see the radial distribution functions presented earlier), only the average potential energy of interaction of *any* waters at a particular distance from a quinone oxygen. All water−water interactions are neglected. At close distances, where no waters were found for any structure, the energy was set to zero.

In order to comment on hydrogen bonding to the quinone oxygens, we use the energetic definition of Jorgensen et al.,[59,101−103] which defines a hydrogen bond as an interaction energy of 2.25 kcal/mol or more. When the plot in Figure 5 is compared with the oxygen−oxygen radial distribution function for *p*-benzosemiquinone anion in Figure 2, it is clear that the "peak" in Figure 5 is the result of very few structures (likely one or two) out of a total of at least 2500. However, it may also be seen that all waters closer than about 3.4 Å to the semiquinone oxygens have interaction energies greater than 2.25 kcal/mol. This distance corresponds very well to the first trough in the radial distribution functions of each molecule shown in Figure 2, implying that the first solvation shell is primarily hydrogen bonded to the semiquinone oxygens. Structural and energetic analysis therefore implies that stronger hydrogen bonding to the oxygens of the semiquinone anions appears to make the largest contribution to hydration free energy differences between the quinones and their semiquinone anions. The different hydration structures around the oxygen atoms for the anions further reflect the calculated trend in hydration free energy differences.

Conclusions

One-electron reductions are fundamental reactions in virtually every subdiscipline of chemistry, yet only recently have one-electron reduction potentials[21,22,82] and potential differences between two different molecules[25,104−106] been calculated from atomic properties of solutes and solvents. This contribution tests a method recently proposed for computing reduction potentials[21,82] by applying the method to the redox indicators *p*-benzoquinone and *p*-duroquinone, as well as chloro-substituted *p*-benzoquinones, in water. The method uses thermodynamic cycles to express the reduction free energy as a sum of the gas-phase reduction free energy and the hydration free energy difference between the neutral molecule and its radical anion (see Scheme 2). The gas-phase reduction free energy is approximated by electron affinities calculated by using the hybrid Hartree−Fock/density-functional (HF/DF) B3LYP/6-311G(3d,p) quantum chemical method, whereas hydration free energy differences were estimated by using free energy perturbation/molecular dynamics (FEP/MD) simulations. An alternative thermodynamic cycle involving the transformation of one neutral molecule into another and one anion into another (see Scheme 3) was also tested to avoid changing molecular charge during the thermodynamic perturbation simulations.

The most accurate computed one-electron reduction potentials are within 10−30 meV of experimental values. The most accurate reduction potential was computed for *p*-benzoquinone ($E^0_{calc} = 4.51$ eV and $E^0_{expt} = 4.52-4.54$ eV), whereas the least accurate reduction potential was obtained for *p*-duroquinone ($E^0_{calc} = 3.99$ eV and $E^0_{expt} = 4.18-4.21$ eV). Errors in electron affinities calculated by using the B3LYP HF/DF method[52] and hydration free energy differences calculated by using FEP/MD simulations are relatively small, so relative magnitudes of calculated electron affinities, hydration free energy differences, and reduction free energies were well reproduced.

The primary difference in hydration structures between the *p*-benzoquinones and their semiquinone anions appears near the quinone oxygens. For example, *p*-benzosemiquinone anion has an average of 3.3 water hydrogens contacting each semiquinone oxygen at an approximate distance of 1.6 Å, whereas an average of 1.7 water hydrogens appear approximately 1.8 Å from each oxygen of *p*-benzoquinone. Quinone oxygen−water hydrogen distances and linear O···H−O geometries are consistent with crystallographic features of hydrogen bonds.[98−100] Energetic analysis also supports the importance of hydrogen bonding of water to the oxygen atoms of the semiquinone anions. Broad peaks in the quinone oxygen−water oxygen radial distribution function for *p*-benzosemiquinone anions near 2.5−2.6 Å and 4.4 Å also suggest that water is more ordered around the anions than it is around the neutral *p*-benzoquinones. Indeed, the peaks near 4.4 Å in the anion oxygen−water oxygen radial distribution functions are not present for the neutral quinones and imply that electrostriction may also contribute to hydration free energy differences between the quinones and their semiquinone anions. None of the quinones or their semiquinone anions display similarly close contacts between other atoms and the atoms of water. Further comparison of hydration structures for the anions of *p*-benzoquinone, *p*-duroquinone, and *p*-chloranil shows that calculated hydration free energy differences display the same trend as the distance for the first peak in quinone oxygen−water hydrogen radial distribution functions. The structural analysis therefore provides compelling evidence for the importance of semiquinone anion contacts with water hydrogens and implies that models of water solvation designed to reproduce hydration free energy differences should somehow incorporate the effects of interactions between solutes and proximate water molecules.

Although the relatively good agreement between experimental and calculated one-electron reduction potentials for substituted *p*-benzoquinones confirms the plausibility of combining thermodynamic cycles with hybrid HF/DF quantum chemical and FEP/MD methods to estimate one-electron reduction potentials, work is underway to extend the method to other types of solute molecules in a variety of solvents and in proteins.

Acknowledgment. The research described in this publication was made possible by the OCAST award for Project No. HN3-

011, from the Oklahoma Center for the Advancement of Science and Technology, computer time provided by the University of Oklahoma's University Computing Services, and grants of supercomputer time from the NSF/National Center for Supercomputing Applications and NSF/Cornell Theory Center. The Cornell Theory Center receives major funding from the National Science Foundation and New York State. Additional funding comes from the Advanced Research Projects Agency, the National Institutes of Health, IBM Corporation, and other members of the center's Corporate Research Institute. We are also grateful for supercomputer time made possible by support from IBM Corporation, Silicon Graphics, Inc. and the University of Oklahoma. We thank the Phillips Petroleum Corporation and the University of Oklahoma Department of Chemistry and Biochemistry for fellowship support for A.K.G. and the Department of Chemistry and Biochemistry for a Graduate Research Assistantship for K.S.R. We are also grateful to Professor Bing M. Fung for his generous donation of computer time.

Supporting Information Available: One table and 23 figures showing comparisons of quinone/semiquinone anion oxygen−water hydrogen radial distribution functions, average potential energy distributions, and partial atomic charges used in MD simulations for the quinones in Table 2 (24 pages). Ordering information is given on any current masthead page.

References and Notes

(1) Bard, A. J.; Faulkner, L. R. *Electrochemical Methods, Fundamentals and Applications*; John Wiley & Sons: New York, 1980.
(2) Clark, W. M. *Oxidation-Reduction Potentials of Organic Systems*; The Williams & Wilkins Co.: Baltimore, 1960.
(3) *Electron Transfer in Inorganic, Organic, and Biological Systems*; Bolton, J. R., Mataga, N., McLendon, G., Eds.; American Chemical Society: Washington, DC, 1991; Vol. 228.
(4) Stryer, L. *Biochemistry;* 3rd ed.; W. H. Freeman & Co.: New York, 1988.
(5) Trumpower, B. L.; Gennis, R. B. *Annu. Rev. Biochem.* **1994**, *63*, 675−716.
(6) Taube, H. *Angew. Chem., Int. Ed. Eng.* **1984**, *23*, 329−339.
(7) *Electron Transfer in Biology and the Solid State. Inorganic Compounds with Unusual Properties*; Johnson, M. K., King, R. B., Kurtz, D. M. J., Kutal, C., Norton, M. L., Scott, R. A., Eds.; American Chemical Society: Washington, DC, 1990; Vol. 226.
(8) Kochi, J. K. *Angew. Chem.* **1988**, *100*, 1331−1370.
(9) Eberson, L. *Electron Transfer Reactions in Organic Chemistry*; Springer-Verlag: Berlin, 1987.
(10) Kebarle, P.; Chowdhury, S. *Chem. Rev.* **1987**, *87*, 513−534.
(11) Shalev, H.; Evans, D. H. *J. Am. Chem. Soc.* **1989**, *111*, 2667−2674, and references therein.
(12) Ruoff, R. S.; Kadish, K. M.; Boulas, P.; Chen, E. C. M. *J. Phys. Chem.* **1995**, *99*, 8843−8850.
(13) Stanton, R. V.; Dixon, S. L.; Merz, K. M., Jr. *J. Phys. Chem.* **1995**, *99*, 10701−10704.
(14) Liu, Z.; Carter, L. I.; Carter, E. A. *J. Phys. Chem.* **1995**, *99*, 4355−4359.
(15) Tuckerman, M.; Laasonen, K.; Sprik, M.; Parrinello, M. *J. Chem. Phys.* **1995**, *103*, 150−155.
(16) Laasonen, K.; Klein, M. L. *J. Am. Chem. Soc.* **1994**, *116*, 11620−11621.
(17) Wesolowski, T. A.; Warshel, A. *J. Phys. Chem.* **1994**, *98*, 5183−5187.
(18) Hartke, B.; Carter, E. A. *J. Chem. Phys.* **1992**, *97*, 6569−6578.
(19) Field, M. J. *J. Phys. Chem.* **1991**, *95*, 5104−5108.
(20) Car, R.; Parrinello, M. *Phys. Rev. Lett.* **1985**, *55*, 2471−2474.
(21) Wheeler, R. A. *J. Am. Chem. Soc.* **1994**, *116*, 11048−11051.
(22) Beveridge, A. J.; Williams, M.; Jenkins, T. C. *J. Chem. Soc., Faraday Trans.* **1996**, *92*, 763−768.
(23) Allen, M. P.; Tildesley, D. J. *Computer Simulation of Liquids*; Clarendon Press: Oxford, 1987.
(24) McCammon, J. A.; Harvey, S. C. *Dynamics of Proteins and Nucleic Acids*; Cambridge University: Cambridge, 1987.
(25) Reynolds, C. A.; King, P. M.; Richards, W. G. *Mol. Phys.* **1992**, *76*, 251−275.
(26) Jorgensen, W. L. *Acc. Chem. Res.* **1989**, *22*, 184−189.
(27) Kollman, P. A. *Chem. Rev.* **1993**, *93*, 2395−2417.
(28) van Gunsteren, W. F.; Berendsen, H. J. C. *Angew. Chem.* **1990**, *102*, 1020−1051.
(29) Beveridge, D. L.; DiCapua, F. M. *Annu. Rev. Biophys. Biophys. Chem.* **1989**, *18*, 431−492.
(30) Straatsma, T. P.; McCammon, J. A. *Annu. Rev. Phys. Chem.* **1992**, *43*, 407−435.
(31) Warshel, A.; Chu, Z. T. In *Structure and Reactivity in Aqueous Solution: Characterization of Chemical and Biological Systems*; American Chemical Society: Washington DC, 1994; Vol. 568, p 71.
(32) Smith, J. G.; Fieser, M. *Reagents for Organic Synthesis*; Wiley-Interscience: New York, 1990; Vol. 12.
(33) Kirmaier, C.; Holten, D. *Photosynth. Res.* **1987**, *13*, 225−260.
(34) *Function of Quinones in Energy Conserving Systems*; Trumpower, B. L., Ed.; Academic: New York, 1982.
(35) *The Chemistry of the Quinonoid Compounds*; Patai, S., Rappoport, Z., Eds.; John Wiley & Sons: Chichester, 1988; Vol. 2, Parts 1 & 2.
(36) Wardman, P. *J. Phys. Chem. Ref. Data* **1989**, *18*, 1637−1711.
(37) Rich, P. R.; Bendall, D. S. *Biochim. Biophys. Acta* **1980**, *592*, 506−518.
(38) Born, M. *Z. Phys.* **1920**, *1*, 45−49.
(39) Rashin, A. A.; Honig, B. *J. Phys. Chem.* **1985**, *89*, 5588−5593.
(40) Jayaram, B.; Fine, F.; Sharp, K.; Honig, B. *J. Phys. Chem.* **1989**, *93*, 4320−4327.
(41) Frisch, M. J.; Trucks, G. W.; Head-Gordon, M.; Gill, P. M. W.; Wong, M. W.; Foresman, J. B.; Johnson, B. G.; Schlegel, H. B.; Robb, M. A.; Replogle, S.; Gomperts, R.; Andres, J. L.; Raghavachari, K.; Binkley, J. S.; Gonzalez, C.; Martin, R. L.; Fox, D. J.; Defrees, D. J.; Baker, J.; Stewart, J. J. P.; Pople, J. A. *GAUSSIAN92/DFT*; Gaussian, Inc.: Pittsburgh, 1992.
(42) Stephens, P. J.; Devlin, F. J.; Frisch, M. J. *J. Phys. Chem.* **1994**, *98*, 11623−11627.
(43) Slater, J. C. *Quantum Theory of Molecules and Solids*; McGraw-Hill: New York, 1974; Vol. 4.
(44) Becke, A. *Phys. Rev. A* **1988**, *38*, 3098−3100.
(45) Vosko, S. H.; Wilk, L.; Nusair, M. *Can. J. Phys.* **1980**, *58*, 1200−1211.
(46) Lee, C.; Yang, W.; Parr, R. G. *Phys. Rev. B* **1988**, *37*, 785−789.
(47) Perdew, J. P. *Phys. Rev. B* **1986**, *33*, 8822−8824.
(48) Becke, A. *J. Chem. Phys.* **1992**, *97*, 9173−9177.
(49) Becke, A. D. *J. Chem. Phys.* **1993**, *98*, 1372−1377.
(50) Bauschlicher, D. W.; Partridge, H. *J. Chem. Phys.* **1995**, *103*, 1788−1791.
(51) Bauschlicher, C. W., Jr. *Chem. Phys. Lett.* **1995**, *246*, 40−44.
(52) Boesch, S. E.; Grafton, A. K.; Wheeler, R. A. *J. Phys. Chem.* **1996**, *100*, 10083−10087.
(53) Chowdhury, S.; Grimsrud, E. P.; Kebarle, P. *J. Phys. Chem.* **1986**, *90*, 2747−2752.
(54) Pearlman, D. A.; Case, D. A.; Caldwell, J. C.; Seibel, G. L.; Singh, U. C.; Weiner, P. K.; Kollman, P. A. *AMBER*; University of San Francisco: San Francisco, CA, 1991.
(55) Berendsen, H. J. C.; Postma, J. P. M.; van Gunsteren, W. F.; DiNola, A.; Haak, J. R. *J. Chem. Phys.* **1984**, *81*, 3684−3690.
(56) Andersen, H. C. *J. Chem. Phys.* **1980**, *72*, 2384−2393.
(57) van Gunsteren, W. F.; Berendsen, H. J. C. *Mol. Phys.* **1977**, *34*, 1311−1327.
(58) Ryckaert, J. P.; Ciccotti, G.; Berendsen, H. J. C. *J. Comput. Phys.* **1977**, *23*, 327−341.
(59) Jorgensen, W. L.; Chandrasekhar, J.; Madura, J. D.; Impey, R. W.; Klein, M. L. *J. Chem. Phys.* **1983**, *79*, 926−935.
(60) Kirkwood, J. G. *J. Chem. Phys.* **1934**, *2*, 351−361.
(61) Beveridge, D. L.; Schnuelle, G. W. *J. Phys. Chem.* **1975**, *79*, 2562−2566.
(62) Davis, M. E.; McCammon, J. A. *Chem. Rev.* **1990**, *90*, 509−521.
(63) Sharp, K. A.; Honig, B. *Annu. Rev. Biophys. Biophys. Chem.* **1990**, *19*, 301−332.
(64) Honig, B.; Sharp, K. A.; Yang, A.-S. *J. Phys. Chem.* **1993**, *97*, 1101−1109.
(65) Belhadj, M.; Alper, H. E.; Levy, R. M. *Chem. Phys. Lett.* **1991**, *179*, 13−20.
(66) Rick, S. W.; Berne, B. J. *J. Am. Chem. Soc.* **1994**, *116*, 3949−3954.
(67) Tironi, L. G.; Sperb, R.; Smith, P. E.; van Gunsteren, W. F. *J. Chem. Phys.* **1995**, *102*, 5451−5459.
(68) Alper, H.; Levy, R. M. *J. Chem. Phys.* **1993**, *99*, 9847−9852.
(69) York, D. M.; Darden, T. A.; Pedersen, L. G. *J. Chem. Phys.* **1993**, *99*, 8345−8348.
(70) Luty, B. A.; Tironi, L. G.; van Gunsteren, W. F. *J. Chem. Phys.* **1995**, *103*, 3014−3021.
(71) Bader, J. S.; Chandler, D. *J. Phys. Chem.* **1992**, *96*, 6423−6427.
(72) Buckner, J. K.; Jorgensen, W. L. *J. Am. Chem. Soc.* **1989**, *111*, 2507−2516.
(73) Hirata, F.; Redfern, P.; Levy, R. M. *Int. J. Quantum Chem., Quantum Biol. Symp.* **1989**, *15*, 179−190.
(74) Chan, S. L.; Lim, C. *J. Phys. Chem.* **1994**, *98*, 692−695.
(75) Weiner, S. J.; Kollman, P. A.; Nguyen, D. T.; Case, D. A. *J. Comput. Chem.* **1986**, *7*, 230−252.

(76) Weiner, S. J.; Kollman, P. A.; Case, D. A.; Singh, U. C.; Ghio, C.; Alagona, G.; Profeta, S.; Weiner, P. *J. Am. Chem. Soc.* **1984**, *106*, 765−784.
(77) Boesch, S. E.; Wheeler, R. A. *J. Phys. Chem.* **1995**, *99*, 8125−8134.
(78) Qin, Y.; Wheeler, R. A. *J. Chem. Phys.* **1994**, *102*, 1689−1698.
(79) Qin, Y.; Wheeler, R. A. *J. Phys. Chem.* **1996**, *100*, 10554−10563.
(80) Walden, S. E.; Wheeler, R. A. *J. Chem. Soc., Perkin Trans. 2* **1996**, 2663−2671.
(81) Grafton, A. K.; Boesch, S. E.; Wheeler, R. A. *J. Mol. Struct.*: *THEOCHEM* **1997**, in press.
(82) Wise, K. E.; Grafton, A. K.; Wheeler, R. A. *J. Phys. Chem.* **1997**, in press.
(83) Wiberg, K. B.; Hadad, C. M.; LePage, T. J.; Breneman, C. M.; Frisch, M. J. *J. Phys. Chem.* **1992**, *96*, 671−679.
(84) Hess, B. A. J.; Schaad, L. J.; Carsky, P.; Zahradnik, R. *Chem. Rev.* **1986**, *86*, 709−730.
(85) Boesch, S. E.; Wheeler, R. A. *J. Phys. Chem.*, in preparation.
(86) Boatz, J. A.; Gordon, M. S. *J. Phys. Chem.* **1989**, *93*, 1819−1826.
(87) Chirlian, L. E.; Francl, M. M. *J. Comput. Chem.* **1987**, *8*, 894−905.
(88) Breneman, C. M.; Wiberg, K. B. *J. Comput. Chem.* **1990**, *11*, 361−373.
(89) Meisel, D.; Fessenden, R. W. *J. Am. Chem. Soc.* **1976**, *98*, 7505−7510.
(90) Meisel, D.; Czapski, G. *J. Phys. Chem.* **1975**, *79*, 1503−1509.
(91) Ilan, Y. A.; Czapski, G.; Meisel, D. *Biochim. Biophys. Acta* **1976**, *430*, 209−224.
(92) Heinis, T.; Chowdhury, S.; Scott, S. L.; Kebarle, P. *J. Am. Chem. Soc.* **1988**, *110*, 400−407.
(93) Fukuda, E. K.; McIver, R. T. *J. Am. Chem. Soc.* **1985**, *107*, 2291−2296.
(94) Trasatti, S. *Pure Appl. Chem.* **1986**, *58*, 956−966.
(95) Note: Hydration free energy differences calculated by using double-wide sampling and thermodynamic cycle in Scheme 2 for *p*-benzoquinone and *p*-duroquinone were 2.60 and 2.35 eV, respectively.
(96) McQuarrie, D. A. *Statistical Mechanics*; Harper & Row: New York, 1976; Chapter 13.
(97) Chandler, D. *Introduction to Modern Statistical Mechanics*; Oxford University: Oxford, 1987; Section 7.2.
(98) Hamilton, W. C.; Ibers, J. A. *Hydrogen Bonding in Solids*; W. A. Benjamin: New York, 1968.
(99) Taylor, R.; Kennard, O. *Acc. Chem. Res.* **1984**, *17*, 320−326.
(100) *The Hydrogen Bond*; Schuster, P., Zundel, G., Sandorfy, C., Eds.; North-Holland: Amsterdam, 1976; Vols I−III.
(101) Jorgensen, W. L. *J. Chem. Phys.* **1982**, *77*, 4156−4163.
(102) Jorgensen, W. L. *J. Am. Chem. Soc.* **1981**, *103*, 335−340.
(103) Chandrasekhar, J.; Jorgensen, W. L. *J. Chem. Phys.* **1982**, *77*, 5080−5089.
(104) Reynolds, C. A.; King, P. M.; Richards, W. G. *Nature* **1988**, *334*, 80−82.
(105) Reynolds, C. A. *J. Am. Chem. Soc.* **1990**, *112*, 7545−7551.
(106) Lister, S. G.; Reynolds, C. A.; Richards, W. G. *Int. J. Quantum Chem.* **1992**, *41*, 293−310.